POLARIZATION RESPONSE FUNCTIONS IN KAON ELECTROPRODUCTION

C. BENNHOLD
Center for Nuclear Studies, Department of Physics
The George Washington University
Washington, D. C. 20052, USA

T. MART, D. KUSNO
Jurusan Fisika, FMIPA, Universitas Indonesia, Depok 16424, Indonesia

The electroproduction of kaons on the nucleon is shown to be an ideal tool to extract electromagnetic form factors of strange mesons and hyperons. Longitudinal $n(e,e'K^0)\Lambda$ cross sections are found to be sensitive to the K^0 form factor, while sensitivity to the Λ magnetic form factor can be seen in recoil-beam double polarization observables. The $KK^*\gamma$ transition form factor could be extracted by measuring transverse response functions in the $K\Sigma$ channels.

1 Structure Functions in Kaon Electroproduction

The recent advancement of TJNAF and other high-duty cycle, continuous beam electron accelerators has sparked increased interest in the form factors of baryons and mesons. Experimental programs have been completed at TJNAF to measure the form factor of the charged pion and the charged kaon, while a number of other approved experiments aim at precise measurements of the proton and neutron form factors. On the theoretical side, the recent advances on improved actions in Lattice Gauge calculations should soon lead to reliable results for strange hadron form factors. However, except for the K^+ no calculation up to now has given a quantitative prediction of the effect of these form factors on experimental observables accessible at these facilities.

In this paper we study the sensitivity of various kaon electroproduction reactions to the electromagnetic form factors of the involved hyperons and mesons. Allowing for polarization in beam, target and recoil, the differential cross section for kaon production with a virtual photon can be written as [1]

$$\begin{aligned}\frac{d\sigma_v}{d\Omega_K} &= \frac{\mid \vec{q}_K \mid}{k_\gamma^{cm}} P_\alpha P_\beta \Big\{ R_T^{\beta\alpha} + \varepsilon_L R_L^{\beta\alpha} + [2\varepsilon_L(1+\varepsilon)]^{\frac{1}{2}} \times \\ &({}^cR_{TL}^{\beta\alpha}\cos\phi_K + {}^sR_{TL}^{\beta\alpha}\sin\phi_K) + \varepsilon({}^cR_{TT}^{\beta\alpha}\cos 2\phi_K + {}^sR_{TT}^{\beta\alpha}\sin 2\phi_K) + \\ &h\,[2\varepsilon_L(1-\varepsilon)]^{\frac{1}{2}}\,({}^cR_{TL'}^{\beta\alpha}\cos\phi_K + {}^sR_{TL'}^{\beta\alpha}\sin\phi_K) + h(1-\varepsilon^2)^{\frac{1}{2}} R_{TT'}^{\beta\alpha} \Big\}, \quad (1)\end{aligned}$$

where $P_\alpha = (1, \vec{P})$ and $P_\beta = (1, \vec{P}')$. Here $\vec{P} = (P_x, P_y, P_z)$ denotes the

Table 1: Complete response functions for the pseudoscalar meson electroproduction [1]. The polarization of the target (recoil) is indicated by α (β). The last three columns (${}^cTL'$, ${}^sTL'$, and TT') are response functions for the polarized electron. ‡ denotes a response function which does not vanish but is identical to another response function.

β	α	T	L	${}^cTL$	${}^sTL$	${}^cTT$	${}^sTT$	${}^cTL'$	${}^sTL'$	TT'
-	-	R_T^{00}	R_L^{00}	R_{TL}^{00}	0	R_{TT}^{00}	0	0	$R_{TL'}^{00}$	0
-	x	0	0	0	R_{TL}^{0x}	0	R_{TT}^{0x}	$R_{TL'}^{0x}$	0	$R_{TT'}^{0x}$
-	y	R_T^{0y}	R_L^{0y}	R_{TL}^{0y}	0	‡	0	0	$R_{TL'}^{0y}$	0
-	z	0	0	0	R_{TL}^{0z}	0	R_{TT}^{0z}	$R_{TL'}^{0z}$	0	$R_{TT'}^{0z}$
x'	-	0	0	0	$R_{TL}^{x'0}$	0	$R_{TT}^{x'0}$	$R_{TL'}^{x'0}$	0	$R_{TT'}^{x'0}$
y'	-	$R_T^{y'0}$	‡	‡	0	‡	0	0	‡	0
z'	-	0	0	0	$R_{TL}^{z'0}$	0	$R_{TT}^{z'0}$	$R_{TL'}^{z'0}$	0	$R_{TT'}^{z'0}$
x'	x	$R_T^{x'x}$	$R_L^{x'x}$	$R_{TL}^{x'x}$	0	‡	0	0	$R_{TL'}^{x'x}$	0
x'	y	0	0	0	‡	0	‡	‡	0	‡
x'	z	$R_T^{x'z}$	$R_L^{x'z}$	‡	0	‡	0	0	‡	0
y'	x	0	0	0	‡	0	‡	‡	0	‡
y'	y	‡	‡	‡	0	‡	0	0	‡	0
y'	z	0	0	0	‡	0	‡	‡	0	‡
z'	x	$R_T^{z'x}$	‡	$R_{TL}^{z'x}$	0	‡	0	0	$R_{TL'}^{z'x}$	0
z'	y	0	0	0	‡	0	‡	‡	0	‡
z'	z	$R_T^{z'z}$	‡	‡	0	‡	0	0	‡	0

target and $\vec{P}' = (P_{x'}, P_{y'}, P_{z'})$ the recoil polarization vector. Due to the self-analyzing property of the hyperon in the final state the kaon electroproduction process is uniquely suited to measure multiple polarization response functions. In total, there are 36 different response functions in any pseudoscalar meson electroproduction experiment [1], listed in Table 1. With a polarized beam already available at TJNAF all of these observables can be accessed once a polarized target is in place. This opens the door for a complete experiment in kaon electroproduction with much less experimental effort than would be required for pion and eta electroproduction.

Over the last several years considerable effort has been spent to develop

models for the electromagnetic production of kaons from nucleons at low energies [2,3,4,5,6]. Due to the limited set of data the various models permit only qualitative conclusions but do not yet allow the extraction of precise coupling constants and resonance parameters. We employ the kaon electroproduction model of Ref. [5] along with the methods of Ref. [6] to extend this model to the $(e, e'K^0)$ channels. Since at present no data are available for the $(e, e'K^0)$ process it is impossible to test the reliability of the above amplitude in this production channel. Therefore, rather than making precise quantitative predictions for counting rates we emphasize here the relative effects that the form factors have on particular response functions.

2 The K^0 Form Factor

Among the SU(3) pseudoscalar mesons, the neutral kaon is the only neutral system that can have a nonvanishing electromagnetic form factor at finite q^2. Invariance of the strong interaction under charge conjugation dictates that the form factors of antiparticles are just the negative of those of the respective particles, thus, the π^0 and η do not have any electromagnetic form factors. Although the strange quark is notably heavier than the up and down quarks, the mass difference is still smaller than the mass scale associated with confinement in Quantum Chromodynamics (QCD), $(m_s - m_d) < \Lambda_{\rm QCD}$. Therefore, if this mass difference affects physical observables, it could lead to a sensitive test of phenomenological models that attempt to describe nonperturbative QCD.

We employ two relativistic quark models to calculate the K^0 form factor, the light-cone quark (LCQ) model [7] and the quark-meson vertex (QMV) model [8]; several recent studies have put forth additional new model calculations of the K^0 electromagnetic form factor [9,10]. The charge form factor of the K^0 meson can be expressed as

$$F_{K^0}(q) \quad = \quad e_d F_L(q) + e_{\bar{s}} F_H(q) \ , \tag{2}$$

where $F_L(q)$ and $F_H(q)$ are two independent form factors generated by the interaction of the photon with the light quark (d) of charge e_d and with the other heavier quark ($\bar{s}$) of charge $e_{\bar{s}}$. The results are compared with predictions from vector meson dominance (VMD) and chiral perturbation theory (χPT). In VMD, we assume that the photon interacts with the strange quark through the ϕ-meson and with the u-and d- quarks through ρ- and ω-mesons, each of them having the strength proportional to the quark charge. By ignoring the mass difference of the ρ- and ω-mesons, we can construct a simple two-pole model of the kaon form factors via $F_L(q) = m_\omega^2/(m_\omega^2 - q^2)$ and $F_H(q) = m_\phi^2/(m_\phi^2 - q^2)$. Using χPT to order p^4, a parameter-free prediction for the K^0 form factor at

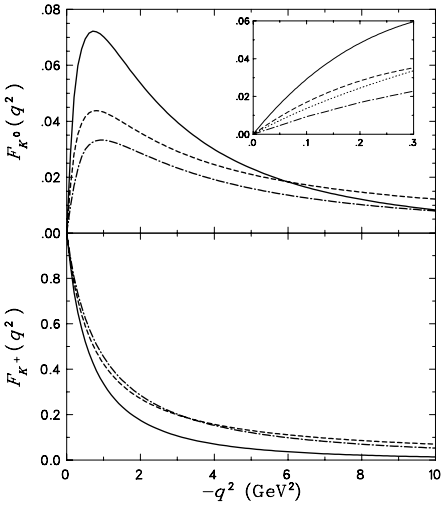

Figure 1: The K^0 and K^+ form factors calculated in the different models. The dash-dotted line represents the QMV calculation, the dashed line shows the VMD model, the dotted line shows the result of χPT, while the solid line comes from LCQ model. The units of the insert are the same as the one for the larger figure.

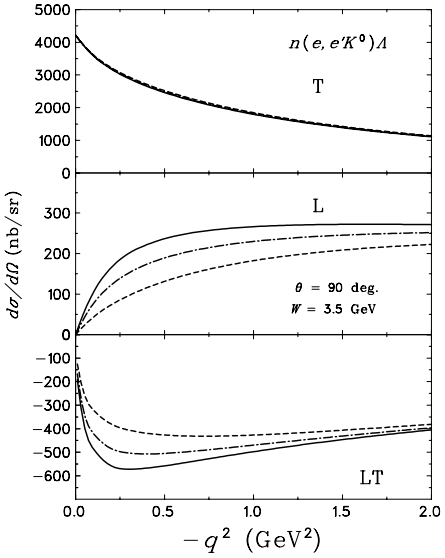

Figure 2: Transverse, longitudinal and longitudinal-transverse cross sections for the $n(e,e'K^0)\Lambda$ process. The solid line shows the calculation with a K^0 form factor obtained in the LCQ model while the dash-dotted line was obtained using the QMV model. The dashed line shows a computation with the K^0 pole excluded.

very low q^2 can be obtained which is due entirely to one-loop diagrams without a tree-level contribution. All models can reproduce the K^+ radius well; the experimental uncertainty of the K^0 radius does not yet distinguish between the different models.

Figure 1 shows the form factors of the neutral kaon calculated in these various models. The charged kaon form factor is shown for comparison. Note that the prediction of χPT is only valid for $-q^2 < 0.3$ GeV^2. The K^0 form factor has a peak around $-q^2 \simeq 1$ GeV^2 for the other three models, though the heights are different. This peak is due to the behavior of the two different form factors, $F_L(q)$ and $F_H(q)$, that define F_{K^0} as shown in Eq. (2). $F_H(q)$ is generated by the coupling of the photon to the heavy quark and, therefore, falls off slower than $F_L(q)$ which comes from the light quark. Once the form factors are weighted by the quark charges, $e_d = -\frac{1}{3}$ and $e_{\bar{s}} = +\frac{1}{3}$, the general shape of F_{K^0} is given.

In Fig. 2 we present predictions for the longitudinal and transverse differential cross section of the $n(e,e'K^0)\Lambda$ reaction using two different quark models for the K^0 form factor. While the transverse response is insensitive to the K^0 pole the longitudinal cross section computed with the form factor obtained from the LCQ-model is almost 50% larger than the calculation with no K^0 pole while the QMV-model calculation lies between those two. The similar sensitivities of the L and LT cross sections indicate that a Rosenbluth separation is not imperative in order to isolate the K^0 form factor effects.

3 The Λ Form Factor

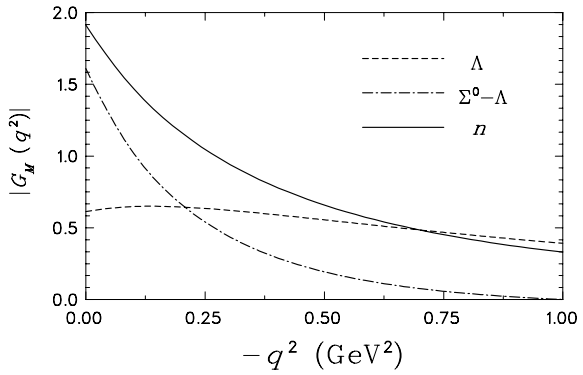

Figure 3: The Λ and $\Lambda-\Sigma^0$ transition magnetic form factors as predicted by Ref.[11] compared with that of the neutron.

Interest in the hyperon electromagnetic form factors is related to the question of SU(3) flavor symmetry breaking and the effects of explicit and hidden strangeness in electromagnetic observables. Applying SU(3) symmetry allows predicting the hyperon form factors in vector meson dominance, quark and soliton models in terms of model parameters fixed by nucleon data. However, there is no direct method of measuring hyperon form factors since there are no stable hyperon targets. Here we suggest that kaon electroproduction may provide at least an indirect method of obtaining information on these form factors. Since the hyperon appears in the u-channel one would want to choose kinematics with small u and large t to suppress t-channel contributions.

Figure 3 shows the Λ magnetic form factor as predicted in Ref.[11]. They used a hybrid vector meson dominance (VMD) formalism which provides a smooth transition from the low-q^2 behavior predicted by vector meson dominance to the high-q^2 scaling of perturbative QCD. The key feature is the

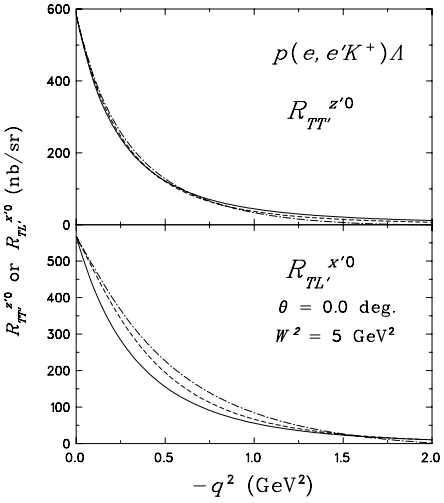

Figure 4: The sensitivity of response functions to different models of the Λ form factor. The solid line corresponds to the neutron magnetic form factor, the dash-dotted line is obtained by using a point-particle approximation, while the dashed line is due to the Λ form factor given by Ref. [11].

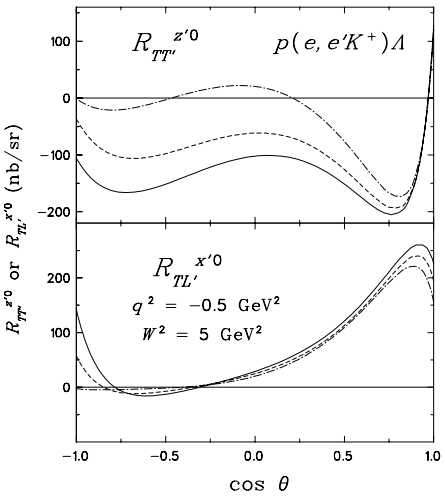

Figure 5: As in Fig. 4, but for different kinematics.

application of the universality limit of the vector meson hadronic coupling SU(3) symmetry relations. Using a direct photon coupling along with a ϕ and ω pole they predict the Λ form factor, while the $\Lambda - \Sigma$ transition form factor is obtained similarly, using a direct photon coupling and a ρ pole. Theoretically, the ratio of these form factors would be interesting since the Λ form factor depends only on isoscalar currents while the $\Lambda - \Sigma$ transition depends only on isovector contributions. Hence, as pointed out in Ref. [11], this ratio might see explicit strangeness and OZI effects such as the suppression or enhancement of effective ρ, ω and ϕ vector meson-hyperon couplings relative to the vector meson-nucleon couplings and SU(3) flavor symmetry predictions. In comparison, we show the neutron magnetic form factor with a simple, standard dipole parametrization. Most previous $(e, e'K)$ studies have used this neutron form factor parametrization for the Λ, scaled by the magnetic moment. Clearly, the q^2-dependence of the Λ form factor predicted by VMD is very different from the shape of the neutron form factor with a much slower fall-off.

Figures 4 and 5 display double polarization response functions for the

$p(e, e'K^+)\Lambda$ reaction that involve beam as well as recoil polarization. These observables were subject of a recent TJNAF proposal [12]. While the TL' response shows moderate sensitivity to the different Λ form factors at very forward and backward angles, the TT' structure function displays large sensitivities over almost the entire angular range, changing both the magnitude and the shape of the cross section. Measuring these response functions could be accomplished with CLAS in TJNAF's Hall B.

4 The $KK^*\gamma$ Transition Form Factor

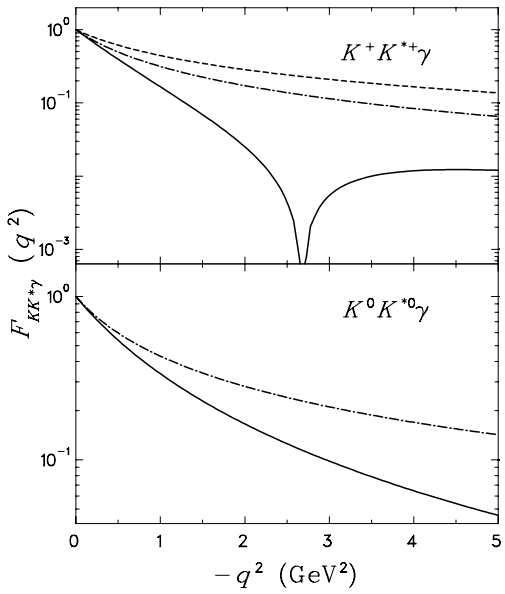

Figure 6: The transition $K^+K^{*+}\gamma$ and $K^0K^{*0}\gamma$ form factors as predicted by Ref. [5] (dash-dotted lines) and Ref. [9] (solid lines).

The $KK^*\gamma$ form factors have not been studied as intensely as their non-strange counterparts, the $\rho\pi\gamma$ and $\omega\pi\gamma$ form factors which are very important in meson exchange current corrections to deuteron electrodisintegration. For the $KK^*\gamma$ transition the form factors are again very sensitive to the mass difference between strange and non-strange quarks. Figure 6 shows the transition form factors for both the neutral and the charged case, comparing the model of Ref. [5] which uses vector meson dominance and the calculation of Ref. [9] which

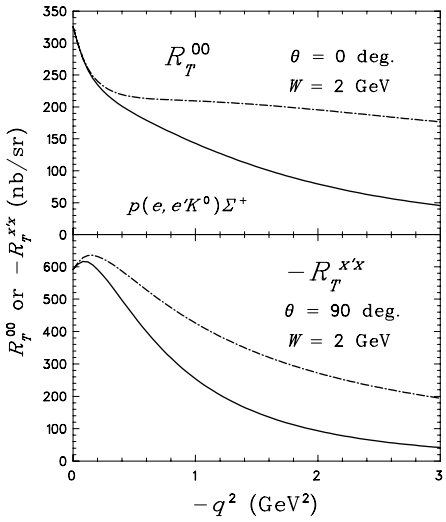

Figure 7: The sensitivity of response functions to different $K^0K^{*0}\gamma$ form factors. The solid (dash-dotted) line is obtained by using the model of Ref. [9] ([5]).

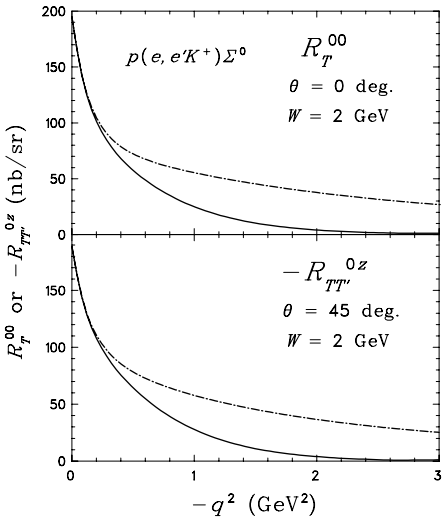

Figure 8: As in Fig. 7, but for the $K^+K^{*+}\gamma$ form factors.

solves a covariant Salpeter equation for a confining plus instanton-induced interaction. Both models fall off faster than the elastic K^+ form factor which is shown for comparison. The form factor in the charged case displays a zero at higher q^2, indicating destructive interference between the light and the heavy quark contribution.

Figures 7 and 8 display the sensitivity of different transverse response functions to the transition form factors. Since the small size of the $g_{K\Sigma N}$ coupling constant suppresses the Born terms the $p(e,e'K^+)\Sigma^0$ reaction is used to study the $K^+K^{*+}\gamma$ form factor while the $p(e,e'K^0)\Sigma^+$ is sensitive to the neutral transition. Questions remain regarding additional t-channel resonance contributions from states like the $K_1(1270)$ which would have a different transition form factor. The observables displayed can clearly distinguish between the different models, with the model of Ref. [9] leading to a much faster fall-off. Unfortunately, the zero in the charged transition form factor around $q^2 = -2.6$ GeV^2 is not visible since the cross sections are already very small at these momentum transfers.

5 Conclusion

In this paper we have shown that the kaon electroproduction process is well suited to extract the form factors of strange mesons and baryons. However, this cannot be done model-independently like a Chew-Low extrapolation in the case of the charged pion or kaon. In order to reduce the model dependency and obtain accurate quantitative predictions one requires the information from the TJNAF kaon photoproduction experiments [13]. The analysis of those measurements should determine the relevant resonances and coupling constants and thus uniquely define the production amplitude.

Acknowledgments

We are grateful to K. Dhuga and O.K. Baker for useful discussions regarding the experimental aspects. This work is supported by the US DOE grant no. DE-FG02-95-ER40907 and the University Research for Graduate Education (URGE) grant.

References

1. G. Knöchlein, D. Drechsel, and L. Tiator, *Z. Phys.* A **352**, 327 (1995).
2. R.A. Adelseck, C. Bennhold, and L.E. Wright, *Phys. Rev.* C **32**, 1681 (1985).
3. J.C. David, C. Fayard, G.H. Lamot, and B. Saghai, *Phys. Rev.* C **53**, 2613 (1996).
4. R.A. Adelseck and B. Saghai, *Phys. Rev.* C **42**, 108 (1990).
5. R.A. Williams, C.-R. Ji, and S.R. Cotanch, *Phys. Rev.* C **46**, 1617 (1992).
6. T. Mart, C. Bennhold, and C.E. Hyde-Wright, *Phys. Rev.* C **51**, R1074 (1995); T. Mart and C. Bennhold, *Nucl. Phys.* A **585**, 369c (1995).
7. C. Bennhold, H. Ito, and T. Mart, *Proceedings of the 7th International Conference on the Structure of Baryons*, Santa Fe, New Mexico, 1995, p.323; *ibid.*, submitted to Phys. Rev. C.
8. W.W. Buck, R. Williams, and H. Ito, *Phys. Lett.* B **351**, 24 (1995); H. Ito and F. Gross, *Phys. Rev. Lett.* **71**, 2555 (1993).
9. C.R. Münz, J. Resag, B.C. Metsch, and H.R. Petry, *Phys. Rev.* C **52**, 2110 (1995).
10. F. Cardarelli, I.L. Grach, I.M. Narodetskii, E. Pace, G. Salmè, and S. Simula, *Phys. Rev.* D **53**, 6682 (1996).

11. R.A. Williams and T.M. Small, *Phys. Rev.* C **55**, 882 (1997); R.A. Williams and C. Puckett-Truman, *Phys. Rev.* C **53**, 1580 (1996).
12. *Polarization Transfer in Kaon Electroproduction*, TJNAF Proposal, O.K. Baker (spokesperson).
13. *Electromagnetic Production of Hyperons*, CEBAF experiment E-89-004, R. Schumacher (spokesperson), and *Study of Kaon Photoproduction on Deuterium*, CEBAF experiment E-89-045, B. Mecking (spokesperson).